

# Universalities in ultracold reactions of alkali-metal polar molecules

Goulven Quémener\* and John L. Bohn

*JILA, University of Colorado, Boulder, Colorado 80309, USA*

Alexander Petrov† and Svetlana Kotochigova

*Temple University, Philadelphia, Pennsylvania 19122, USA*

(Received 18 August 2011; published 2 December 2011)

We consider ultracold collisions of ground-state heteronuclear alkali-metal dimers that are susceptible to four-center chemical reactions  $2AB \rightarrow A_2 + B_2$  even at submicrokelvin temperatures. These reactions depend strongly on species, temperature, electric field, and confinement in an optical lattice. We calculate *ab initio* van der Waals coefficients for these interactions and use a quantum formalism to study the scattering properties of such molecules under an external electric field and optical lattice. We also apply a quantum threshold model to explore the dependence of reaction rates on the various parameters. We find that, among the heteronuclear alkali-metal fermionic species, LiNa is the least reactive, whereas LiCs is the most reactive. For the bosonic species, LiK is the most reactive in zero field, but all species considered, LiNa, LiK, LiRb, LiCs, and KRb, share a universal reaction rate once a sufficiently high electric field is applied. For indistinguishable bosons, the inelastic/reactive rate increases as  $d^2$  in the quantum regime, where  $d$  is the dipole moment induced by the electric field. This is a weaker power-law dependence than for indistinguishable fermions, for which the rate behaves as  $d^6$ .

DOI: [10.1103/PhysRevA.84.062703](https://doi.org/10.1103/PhysRevA.84.062703)

PACS number(s): 34.50.Cx

## I. INTRODUCTION

The study of ultracold polar molecules has become a vast and exciting area of interest since the formation of bi-alkali-metal heteronuclear polar molecules [1–5]. The molecules can be controlled at the ground electronic, vibrational, rotational [3], and hyperfine [6] quantum level. The external motion of the polar molecules can also be modified by an electric field [7] and by optical lattice confinement [8].

Polar molecules offer remarkable characteristics. First, they have strong electric dipole moments [9,10]. The interactions between polar molecules can then be dominated by electric dipole-dipole terms. The electric molecular interactions are strong, long-range, anisotropic, and can be tuned by electric fields more readily than for atoms [11,12]. Second, the polar molecules can be either bosons or fermions. If the polar molecules are addressed in a single quantum state, they become indistinguishable and quantum statistics plays a strong role. An ultracold gas of bosonic molecules can lead to Bose-Einstein condensation, and an ultracold sample of fermionic molecules can lead to a degenerate Fermi gas. Third, two polar molecules can be reactive or not [13–16]. It was found in Ref. [13] that, among the bi-alkali-metal heteronuclear molecules in their absolute fundamental ground state, the lithium species LiNa, LiK, LiRb, and LiCs in addition to the KRb molecule (category 1) gave rise to two-body exoergic chemical reactive processes while the remaining species NaK, NaRb, NaCs, KCs, and RbCs (category 2) resulted in two-body endoergic processes. Reactivity is an advantage in investigating the ultracold chemistry of molecules [17]. It also provides a clear signature (in term of molecular

loss) of two-body interactions in a gas and depends strongly on the applied electric field [18]. The nonreactive molecules have the advantage of being chemically stable in their absolute ground state and can help in reaching long-lived samples of polar molecules. However, if dense samples of molecules are formed in Bose-Einstein condensates for example, three-body collision can become a source of loss, and it is important to investigate the collisional properties of such processes [19–21]. Finally, molecules offer a rich internal quantum structure and can be manipulated with electromagnetic waves in order to address their quantum states. Exciting perspectives have been proposed for these polar molecules, involving condensed matter and many-body physics, quantum magnetism, precision measurements, controlled chemistry, and quantum information [22–28].

For all these reasons, many experimental groups are currently interested in creating polar molecules. The fermionic polar molecules  $^{40}\text{K}^{87}\text{Rb}$  has received particular experimental [3,6–8,17,29] and theoretical [18,30–40] consideration recently. However, much less is known about the interactions and the dynamical properties of the other polar bi-alkali-metal molecules, to which experimental attention is also devoted [1,2,4,41–49]. This is what we address in this paper. In Sec. II, we compute the isotropic long-range van der Waals coefficients between polar molecules. We focus our study on the exoergic molecules (category 1). In Sec. III, we use these parameters to perform quantum scattering calculations assuming full loss when the polar molecules are close to each other. We consider the case of collisions in free and confined space, in electric fields. We use a quantum threshold (QT) model to explain how the collisional properties scale with the different species. We arrive at analytical expressions for high-loss collision rates of bosonic or fermionic molecules, which can also be applied to the inelastic and reactive case of molecules of category 2, as well as atom-atom or atom-molecule collisions, provided the van der Waals coefficients are known. We conclude in Sec. IV.

\*goulven.quemener@colorado.edu

†On leave from St. Petersburg Nuclear Physics Institute, Gatchina, 188300 Russia and St. Petersburg State University, St. Petersburg, 198904 Russia.

## II. ISOTROPIC LONG-RANGE INTERACTION OF REACTIVE POLAR MOLECULES

The isotropic dispersion coefficient  $C_6$  between two identical diatomic alkali-metal molecules in the  $v = 0$  and  $J = 0$  rovibrational ground state of the  $X^1\Sigma^+$  potential has three contributions:

$$C_6 = C_6^{(\text{gr})} + C_6^{(\text{exc})} + C_6^{(\text{inf})} = \frac{3}{\pi} \int_0^\infty d\omega \left\{ \alpha_{\text{gr}}^2(i\omega) + \alpha_{\text{exc}}^2(i\omega) + 2\alpha_{\text{gr}}(i\omega)\alpha_{\text{exc}}(i\omega) \right\}, \quad (1)$$

where the first term of the integrand is the square of the isotropic dynamic polarizability  $\alpha_{\text{gr}}(i\omega)$  at imaginary frequency  $i\omega$  due to rovibrational transitions within the ground-state potential. The second term in the integrand is the square of the isotropic polarizability  $\alpha_{\text{exc}}(i\omega)$  due to transitions to the rovibrational levels of electronically excited potentials, while the last term indicates an interference between the first two contributions. In these and subsequent expressions, both the dispersion coefficient and the polarizability are in atomic units. A thorough discussion of dispersion forces between molecules can be found in Ref. [50].

We find that  $\alpha_{\text{gr}}(i\omega) = \alpha_{0g}/[1 + (\omega/\eta_g)^2]$  [50,51] to a good approximation with  $\alpha_{0g} = d_p^2/(3B)$  and  $\eta_g = 2B$ , where  $d_p$  and  $B$  are respectively the electric permanent dipole moment and rotational constant at the equilibrium separation  $R_e$  between the atoms in the molecule. The contribution from transitions between vibrational levels within the ground-state potential is negligibly small. Consequently,  $C_6^{(\text{gr})} = d_p^4/(6B)$  in agreement with the findings of Ref. [52].

The isotropic dynamic polarizability  $\alpha_{\text{exc}}(i\omega)$  contains contributions from transitions to the rovibrational excited  $^1\Sigma^+$  and  $^1\Pi$  potentials, which correspond to the parallel and perpendicular components of the polarizability, respectively. Based on the Franck-Condon principle, we can evaluate the polarizability at each interatomic separation rather than performing an average over rovibrational levels [53]. For  $v = 0$  and  $J = 0$  the separation is  $R = R_e$ . We then parametrize  $\alpha_{\text{exc}}(i\omega) = \sum_j \alpha_j(i\omega)$  with

$$\alpha_j(i\omega) = \frac{\alpha_{0j}}{1 + (\omega/\eta_j)^2}. \quad (2)$$

Each term corresponds to an excited potential. In practice, we have found it more convenient to evaluate the polarizability at  $R = R_e$  as a function of real frequencies and find the parameters  $\alpha_{0j}$  and  $\eta_j$  from a fit. The static polarization due to the excited-state potentials is  $\alpha_{\text{exc}}(0) = \sum_j \alpha_{0j}$ . Using Eqs. (1) and (2), we obtain the  $C_6^{(\text{exc})}$  and  $C_6^{(\text{inf})}$  coefficients as

$$C_6^{(\text{exc})} = \frac{3}{2} \sum_{jk} \frac{\alpha_{0j}\alpha_{0k}}{1/\eta_j + 1/\eta_k}, \quad (3)$$

$$C_6^{(\text{inf})} = 3 \sum_j \frac{\alpha_{0g}\alpha_{0j}}{1/\eta_g + 1/\eta_j}. \quad (4)$$

The dynamic polarizability  $\alpha_{\text{exc}}(\omega)$  at real frequency is calculated using a coupled-cluster method with single and double excitations (ccsd) [54]. The calculation of the static polarizability and permanent dipole moment is performed at much higher level using the coupled-cluster method with the

single, double, and triple excitations (ccsdT). Twelve electrons, including  $1s^2 2s^1$  of the Li atom and  $(n-1)s^2(n-1)p^6ns^1$  of the Na, K, Rb, and Cs atoms, were explicitly used in both ccsd and ccsdT calculations. The dipole moment for each molecule was averaged on the zero vibrational level. We employed the correlation-consistent polarized valence-only quadruple-zeta (cc-pCVQZ) basis sets for Li and Na from Refs. [55,56], the all-electron basis for the K atom from Ref. [57], and the effective core potential multiconfigurational Dirac-Fock calculation ECP28MDF and ECP46MDF basis sets with the relativistic effective core potentials from Ref. [58] for the Rb and Cs atoms. A comparison of our data on the dipole moment and static polarizability with results of Refs. [9,10] shows a good agreement within a few percent.

Table I lists our  $C_6$  coefficients for four pairs of identical alkali-metal molecules in the  $v = 0$ ,  $J = 0$  rovibrational level of the  $X^1\Sigma^+$  potential. For completeness, we tabulate the contribution to the isotropic component of the static polarizability from electronically excited potentials, the rotational constant, and the permanent dipole moment for each of the four molecules.

Table I shows that the value of the  $C_6$  coefficient as well as the three contributions to it increase when we move down along the first column of the periodic table for the second atom in our four diatomic molecules. Most of the increase can be traced back to increasing permanent and transition dipole moments. For example, the ground-state contribution  $C_6^{(\text{gr})}$  increases by four orders of magnitude as the permanent dipole moment increases by a factor of 10. For the excited-state contribution  $C_6^{(\text{exc})}$  the increase is less dramatic as the transition dipole moments increase only weakly. Only for the LiNa molecule does the excited-state contribution dominate the  $C_6$  coefficient.

TABLE I. van der Waals  $C_6$  coefficients in atomic units for the interaction between the two molecules in the  $v = 0$ ,  $J = 0$  rovibrational levels of the  $X^1\Sigma^+$  potential and other molecular characteristics used to calculate  $C_6$ ;  $\alpha_{\text{exc}}(0)$  is the isotropic static polarizability due to transitions to electronically excited potentials;  $B$  and  $d_p$  are the rotational constant and electric permanent dipole moment, respectively. These three properties are evaluated at the equilibrium separation  $R_e$ . The value of  $B$  is from Ref. [10]. The next three columns are the excited-state, interference, and ground-state contributions to the total  $C_6$ , shown in the last column.

$\alpha_{\text{exc}}(0)$ (a.u.)	$B/hc$ ( $\text{cm}^{-1}$ )	$d_p$ (D)	$C_6^{(\text{exc})}$ (a.u.)	$C_6^{(\text{inf})}$ (a.u.)	$C_6^{(\text{gr})}$ (a.u.)	$C_6$ (a.u.)
LiNa + LiNa						
237.8	0.377	0.557 <sup>a</sup>	3673	23	222	3917
		0.531 <sup>b</sup>	3673	21	186	3880
LiK + LiK						
324.9	0.258	3.556 <sup>a</sup>	6269	1271	542000	550000
		3.513 <sup>b</sup>	6269	1241	517000	524000
LiRb + LiRb						
346.2	0.220	4.130 <sup>a</sup>	6323	1829	1160000	1170000
		4.046 <sup>b</sup>	6323	1754	1070000	1070000
LiCs + LiCs						
389.7	0.188	5.478 <sup>a</sup>	7712	3620	4200000	4210000
		5.355 <sup>b</sup>	7712	3460	3830000	3840000

<sup>a</sup>Reference [9].

<sup>b</sup>This work.

### III. DYNAMICS IN THREE-DIMENSIONAL SPACE

#### A. Quantum numerical calculation

We use the isotropic van der Waals  $C_6$  coefficients calculated in the previous section to compute the chemical rate coefficients of the reactive polar molecules. We use the same formalism used in Ref. [7] for the chemical reaction  $\text{KRb} + \text{KRb} \rightarrow \text{K}_2 + \text{Rb}_2$ . We employ a time-independent quantum formalism, including only one molecule-molecule channel corresponding to the initial state of the molecules, but including several partial waves. For two particles of masses  $m_1, m_2$ , the Hamiltonian of the system is given by

$$H = T + V_{\text{abs}} + V_{\text{vdW}} + V_{\text{dd}}. \quad (5)$$

Using spherical coordinates  $(r, \theta, \phi)$ , the kinetic energy is  $T = -\hbar^2 \nabla_R^2 / (2\mu)$ ,  $\mu = m_1 m_2 / (m_1 + m_2)$  is the reduced mass of the colliding system,  $V_{\text{abs}} = i A e^{-(r-r_{\text{min}})/r_c}$  is an absorbing potential to account for the loss of particles due to chemical reactions or inelastic collisions in the incident channel, where  $A$  is the strength of the absorbing potential,  $r_{\text{min}}$  is the position where the potential starts, and  $r_c$  is the position where the potential vanishes exponentially.  $V_{\text{vdW}} = -C_6/R^6$  is an isotropic van der Waals interaction, and  $V_{\text{dd}} = [d_1 d_2 (1 - 3 \cos^2 \theta)] / (4\pi \epsilon_0 R^3)$  is the dipole-dipole interaction between the two particles if an electric field is applied. Here  $d_1, d_2$  are the induced electric dipole moments in the laboratory frame and their maximum value is given by their permanent dipole moments  $d_{p,1}, d_{p,2}$  in the molecular frame. We expand the total wave function onto a basis set of spherical harmonics (or partial waves)

$$\Psi^{M_L}(R, \theta, \varphi) = \frac{1}{R} \sum_{L'} Y_{L'}^{M_L}(R, \theta) F_{L'}^{M_L}(R), \quad (6)$$

where  $L$  is the quantum number associated with the orbital angular momentum of the collision, and  $M_L$  the quantum number associated with its projection onto a quantization axis (see Ref. [18] for details). Solution of the eigenstates of the Hamiltonian leads to the set of close-coupling equations

$$\left\{ -\frac{\hbar^2}{2\mu} \frac{d^2}{dR^2} + V_{\text{eff}} + V_{\text{abs}} - E \right\} F_{LL}^{M_L}(R) + \sum_{L' \neq L} -\frac{C_3(L, L'; M_L)}{R^3} F_{LL'}^{M_L}(R) = 0. \quad (7)$$

$E$  represents the total energy which is, in this study, the collision energy  $E_c$ , as we use only one molecule-molecule incident channel. We use the same notation as in Ref. [18]  $C_3(L, L'; M_L) = \alpha_{L, L'}^{M_L} d_1 d_2 / 4\pi \epsilon_0$  with

$$\alpha_{L, L'}^{M_L} = 2(-1)^{M_L} \sqrt{2L+1} \sqrt{2L'+1} \begin{pmatrix} L & 2 & L' \\ 0 & 0 & 0 \end{pmatrix} \times \begin{pmatrix} L & 2 & L' \\ -M_L & 0 & M_L' \end{pmatrix} \delta_{M_L, M_L'}. \quad (8)$$

The effective potential in Eq. (7) is given by

$$V_{\text{eff}} = \frac{\hbar^2 L(L+1)}{2\mu R^2} - \frac{C_6}{R^6} - \frac{C_3(L, L; M_L)}{R^3} \quad (9)$$

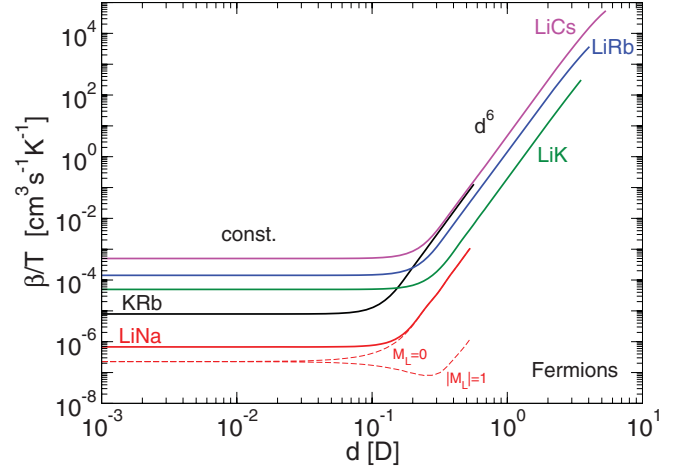


FIG. 1. (Color online) Solid lines: Loss rate coefficient  $\beta_{L=1}$  divided by  $T$  in free three-dimensional (3D) space, of the reaction  $AB + AB \rightarrow A_2 + B_2$  for different reactive fermionic polar molecules ( $AB = \text{LiNa}, \text{KRb}, \text{LiK}, \text{LiRb}, \text{LiCs}$ ), as a function of the electric dipole moment. The fermions are considered in the same indistinguishable quantum state. In the van der Waals regime, the rate coefficient is constant, while in the electric field regime, the rate coefficient behaves as  $d^6$  (see text for details). Dashed lines:  $\beta_{L=1, M_L=0}$  and  $\beta_{L=1, |M_L|=1}$  components of  $L = 1$ , shown here for  $AB = \text{LiNa}$ .

for a given  $L, M_L$ . The absorbing potential is chosen in Eq. (7) in such a way that the loss probability is unity when the two molecules come close together. For such conditions, it turns out that the cross sections and rate coefficients do not depend on the short-range physics phase shift and the position where the propagation starts [31]. The case for which the loss probability is smaller than unity has been discussed in Refs. [31, 33, 36].

We report in Figs. 1 and 2 as solid lines, the loss rate coefficient as a function of the induced electric dipole moment  $d$ , for two indistinguishable fermionic molecules (Fig. 1)

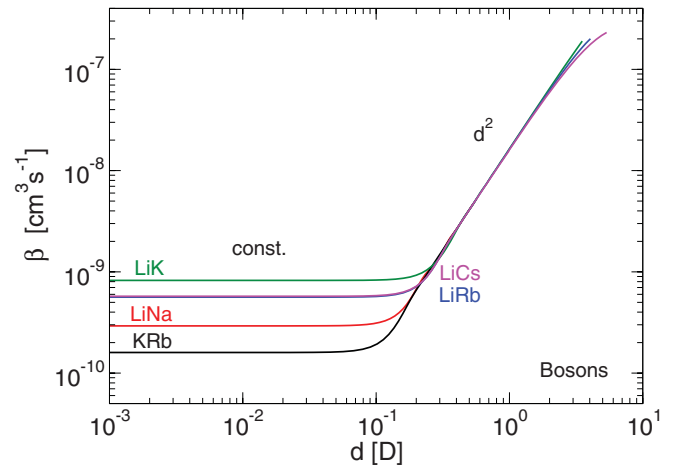


FIG. 2. (Color online) As Fig. 1 for different reactive bosonic polar molecules. The rate coefficient  $\beta_{L=0}$  is plotted as a function of the electric dipole moment for  $T \rightarrow 0$  (Wigner regime). The bosons are considered in the same indistinguishable quantum state. In the van der Waals regime, the rate is constant, while in the electric field regime, the rate coefficient behaves as  $d^2$  (see text for details).

and for two indistinguishable bosonic molecules (Fig. 2), for LiNa-LiNa, KRb-KRb, LiK-LiK, LiRb-LiRb, and LiCs-LiCs collisions. The rate coefficient is defined as in Eq. (7) of Ref. [18]. Note that for fermionic  $p$ -wave collisions ( $L = 1$ ), the curves are the sum of the rate coefficients for  $M_L = 0$  and twice the rate for  $|M_L| = 1$  (to account for  $M_L = +1$  and  $M_L = -1$ ), as illustrated for fermionic LiNa molecules in dashed lines in Fig. 1. To converge the results, we use five partial waves,  $L = 1, 3, 5, 7, 9$  for the fermions and  $L = 0, 2, 4, 6, 8$  for the bosons. We used the values of  $C_6$  and  $d_p$  reported in Table I, and the values of  $C_6 = 16133$  a.u. of Ref. [33] and  $d_p = 0.566$  D of Ref. [3] for KRb. We provide a list of the fermionic and bosonic isotopes of each species in Appendix A. These results were obtained in the regime of ultracold temperature. In this regime, the fermionic rate scales linearly with the temperature (hence we have plotted the rate divided by the temperature) while the bosonic rate is independent of the temperature according to the Bethe-Wigner laws [59,60]. For both cases, the rate scales as a constant in the van der Waals regime where  $d \rightarrow 0$  and is an increasing term in the electric field regime where  $d \rightarrow d_p$ . The transition from the van der Waals regime to the electric field regime occurs for dipole moments around several tenths of one debye. For most bi-alkali-metal molecules, this corresponds to applied electric fields of several tens of kV/cm [61]. We note that, for large dipole moments, the corresponding dipole length  $a_{dd} = \mu d^2 / \hbar^2$  may exceed the distance between molecules given by the inverse third of the molecular gas density  $a_{mm} = n^{-1/3}$ . In such situations, there are no more collisions between molecules. Instead, a dense liquid or solid phase is entered where many-body physics becomes important.

For the fermionic case, in the van der Waals regime, it is seen that the LiNa system is the least reactive, followed by KRb, LiK, LiRb, and finally LiCs. Qualitatively, light masses and small values of  $C_6$  increase the incident  $p$ -wave barrier (this is the case for LiNa) and hence decrease the chance to get high chemical reactivity, while heavy masses and large values of  $C_6$  decrease the barrier (this is the case for LiCs) and increase the reactivity. In the electric field regime, the same general trend is observed, except now the rate of the KRb system is as high as that of the LiCs system. Now the rates seem to scale with the reduced mass of the system only. For a given dipole, the electric dipole interaction is the same between the species; only the centrifugal terms differ. Higher mass means a smaller barrier and so a higher loss rate.

For the bosonic case, in the van der Waals regime, KRb molecules are the least reactive, followed by LiNa, LiRb, LiCs, and finally LiK. Bosonic particles collide in an  $s$  wave at ultralow energy where no incident barrier is present. Instead, one must invoke the probability for quantum transmission. In the electric field regime, all the different systems have the same rate coefficients. This will be explained in the next section.

## B. Quantum threshold model

To understand the physical trends seen in the numerical results, we employ an analytical quantum threshold model [18] which provides a universal expression of an ultracold collision (chemical reaction or inelastic collision) with short-range unit-loss probability. The QT model is a clear and simple model to

describe the dependence of an ultracold chemical reaction on the reduced mass and the isotropic van der Waals  $C_6$  coefficient of the molecule-molecule complex, and on the induced dipole moment via the presence of an applied electric field. The QT model assumes that the loss probability scales as

$$P_{L,M_L} = p_{L,|M_L|} \left\{ \frac{E_c}{E_*} \right\}^{L+1/2}, \quad (10)$$

where  $E_*$  is a characteristic energy corresponding to the long-range interaction of the molecules in a partial wave  $L, M_L$ .  $p_{L,|M_L|}$  is a dimensionless quantity of order unity and is estimated by fitting the expression with the numerical results. The thermalized rate coefficient is expressed by

$$\beta_{L,M_L} = p_{L,|M_L|} \frac{\hbar^2 \pi}{\sqrt{2\mu^3}} \frac{\langle E_c^L \rangle}{E_*^{L+1/2}} \Delta \quad (11)$$

where the angular brackets denote a Maxwell-Boltzmann distribution over the collision energy to the power  $L$ .  $\Delta = 2$  if the particles are in indistinguishable states and 1 if they are in distinguishable states [62].

### 1. QT model for $p$ -wave collisions

For  $p$ -wave collisions ( $L = 1$ ), we chose the characteristic energy  $E_*$  equal to the height of the incident barrier,  $E_{L,|M_L|}^{n,m}$ , of the effective potential  $V_{\text{eff}}$ , composed of the strongest attractive potential  $-C_n/R^n$  and the strongest repulsive potential  $C_m/R^m$ ,

$$E_{L,|M_L|}^{n,m} = \frac{C_m \left( \frac{n C_n}{m C_m} \right)^{n/(n-m)} - C_n \left( \frac{n C_n}{m C_m} \right)^{m/(n-m)}}{\left( \frac{n C_n}{m C_m} \right)^{(n+m)/(n-m)}}. \quad (12)$$

The position of the barrier is given by

$$R_{L,|M_L|}^{n,m} = \left( \frac{n C_n}{m C_m} \right)^{1/(n-m)}. \quad (13)$$

The combinations of  $n$  and  $m$  are given in Table II with the corresponding height of the barriers. For the van der Waals regime and for either  $|M_L| = 0$  or 1, the height of the barrier is made by the attractive van der Waals interaction  $-C_6/R^6$  and the repulsive centrifugal term  $C_2/R^2 \equiv \hbar^2 L(L+1)/(2\mu R^2)$  with  $L = 1$ , giving rise to a characteristic energy  $E_{1,(0,1)}^{6,2}$ . For the electric field regime and for  $|M_L| = 0$ , the height of the barrier is made by the attractive dipole-dipole interaction  $-C_3(1,1;0)/R^3 \equiv -[(4/5)d^2/(4\pi\epsilon_0)]/R^3$  and the repulsive centrifugal term  $C_2/R^2 \equiv \hbar^2 L(L+1)/(2\mu R^2)$  with  $L = 1$ , giving rise to a characteristic energy  $E_{1,0}^{3,2}$ . Finally, for the electric field regime

TABLE II. Characteristic energies  $E_*$  for  $L = 1, |M_L| = 0, 1$  in the van der Waals (vdW) and electric regimes.

Regime	$ M_L $	$-C_n/R^n$	$C_m/R^m$	$E_{L=1, M_L }^{n,m}$
vdW	0,1	$-\frac{C_6}{R^6}$	$\frac{\hbar^2 L(L+1)}{2\mu R^2}$	$\left( \frac{8\hbar^6}{54\mu^3 C_6} \right)^{1/2}$
Electric	0	$-\frac{(4/5)d^2}{4\pi\epsilon_0 R^3}$	$\frac{\hbar^2 L(L+1)}{2\mu R^2}$	$\frac{25\hbar^6}{108\mu^3} \left( \frac{d^2}{4\pi\epsilon_0} \right)^{-2}$
Electric	1	$-\frac{72\mu d^4}{875\hbar^2(4\pi\epsilon_0)^2 R^4}$	$\frac{(2/5)d^2}{4\pi\epsilon_0 R^3}$	$\frac{(875/24)^3 \hbar^6}{10000\mu^3} \left( \frac{d^2}{4\pi\epsilon_0} \right)^{-2}$

and for  $|M_L| = 1$ , the height of the barrier is made by an attractive  $-C_4/R^4 \equiv -\{[72 \mu/(875 \hbar^2)] d^4/(4\pi \epsilon_0)^2\}/R^4$  and the repulsive dipole-dipole interaction  $-C_3(1, 1)/R^3 \equiv +[(2/5) d^2/(4\pi \epsilon_0)]/R^3$ , giving rise to a characteristic energy  $E_{1,1}^{4,3}$ . The  $-C_4/R^4$  attractive interaction comes from the coupling between the  $L = 1$  and  $L = 3$  parts of the  $|M_L| = 1$  component. This is demonstrated in Appendix B.

Substituting these three values of  $E_*$  into Eq. (11) for  $L = 1$  and assuming  $\langle E_c \rangle = 3k_B T/2$ , where  $k_B$  is the Boltzmann constant and  $T$  the temperature, we arrive at the following expressions for the  $|M_L| = 0, 1$  rate as  $d \rightarrow 0$  in the van der Waals regime:

$$\beta_{L=1, |M_L|=0, 1}^{\text{vdW}} = p_{1,(0,1)}^{6,2} \frac{\pi}{8} \left( \frac{3^{13} \mu^3 C_6^3}{\hbar^{10}} \right)^{1/4} k_B T \Delta \quad (14)$$

with

$$p_{1,(0,1)}^{6,2} = 0.53 \pm 0.07. \quad (15)$$

The  $|M_L| = 0$  rate as  $d \rightarrow d_p$  in the electric field regime is

$$\beta_{L=1, |M_L|=0}^{\text{elec}} = p_{1,0}^{3,2} \frac{3\pi}{8} \left( \frac{6^9}{5^6} \right)^{1/2} \frac{\mu^3}{\hbar^7} \frac{d^6}{(4\pi \epsilon_0)^3} k_B T \Delta \quad (16)$$

with

$$p_{1,0}^{3,2} = 0.54 \pm 0.04. \quad (17)$$

Finally, the  $|M_L| = 1$  rate as  $d \rightarrow d_p$  in the electric field regime is given by

$$\beta_{L=1, |M_L|=1}^{\text{elec}} = p_{1,1}^{4,3} \frac{3\pi}{8} [20\,000(24/875)^3]^{3/2} \frac{\mu^3}{\hbar^7} \frac{d^6}{(4\pi \epsilon_0)^3} k_B T \times \Delta \quad (18)$$

with

$$p_{1,1}^{4,3} = 0.16 \pm 0.02. \quad (19)$$

The coefficients  $p_{L, |M_L|}^{n,m}$  associated with the characteristic energies  $E_{L, |M_L|}^{n,m}$  are found by confronting the analytical results in Eqs. (14), (16), and (18) with our numerical calculations of Fig. 1. The quantity  $\beta_{L=1, |M_L|=0, 1}^{\text{vdW}}$  divided by  $T$  obtained from the numerical results is plotted as a function of the quantity  $(\mu C_6)^{3/4}$  for the van der Waals regime in the top panel of Fig. 3. The quantities  $\beta_{L=1, |M_L|=0}^{\text{elec}}$  and  $\beta_{L=1, |M_L|=1}^{\text{elec}}$  divided by  $d^6$  and  $T$  are plotted as functions of the quantity  $\mu^3$  for the electric field regime for the  $|M_L| = 0$  and  $|M_L| = 1$  components in the middle and bottom panels of Fig. 3, respectively, for the different fermionic reactive systems. We find that the numerical results fit a line, confirming the validity of the QT model analysis (the fitting uncertainty of the lines provides an uncertainty to the  $p_{L, |M_L|}^{n,m}$  parameters). The fitting parameters are the slopes of these lines and are reported in Eqs. (15), (17), and (19).

We see that the analytical rates [Eq. (14)] of both components  $|M_L| = 0, 1$  at ultracold temperature are the same in the van der Waals regime and are dictated by a  $d^6$  dependence in the electric regime [Eqs. (16) and (18)] with different magnitudes. These expressions provide a clear explanation of the trends observed numerically. The loss rate behaves as  $(\mu C_6)^{3/4}$  in the van der Waals regime. In the electric field regime, the loss rate scales as  $\mu^3$ , increasing only with

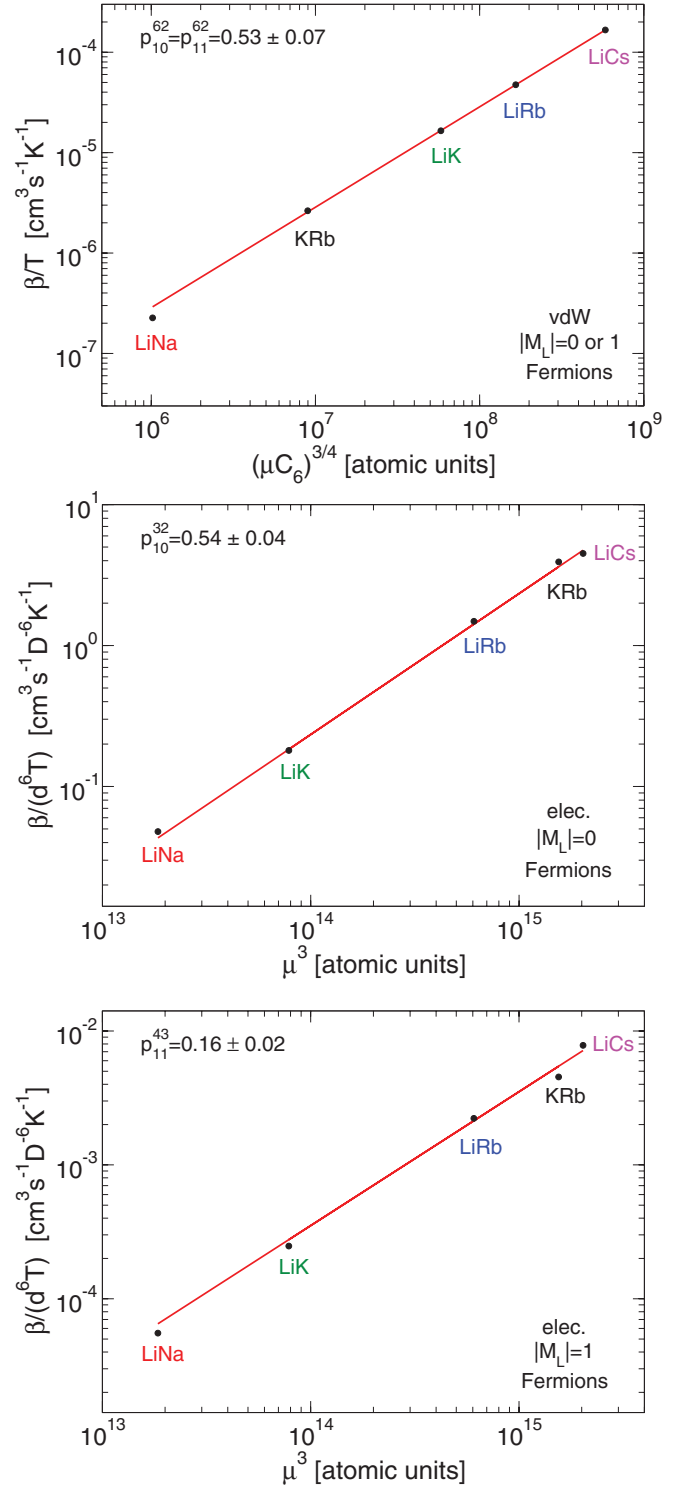


FIG. 3. (Color online) Top panel: Van der Waals regime for  $M_L = 0$  and  $|M_L| = 1$ . The quantity  $\beta_{1,0}^{6,2} = \beta_{1,1}^{6,2}$  divided by  $T$  is plotted as a function of  $(\mu C_6)^{3/4}$ . Middle panel: Electric field regime for  $M_L = 0$ . The quantity  $\beta_{1,0}^{3,2}$  divided by  $d^6 T$  is plotted as a function of  $\mu^3$ . Bottom panel: Electric field regime for  $|M_L| = 1$ . The quantity  $\beta_{1,1}^{4,3}$  divided by  $d^6 T$  is plotted as a function of  $\mu^3$ .

the mass. In both regimes, these expressions explain why fermionic LiNa is the least reactive and fermionic LiCs the most reactive alkali-metal polar species.

We note that the result of  $p_{1,(0,1)}^{6,2} = 0.53 \pm 0.07$  is in very good agreement with the analytical expression of  $2^{19/4} \pi / \{3^{17/4} [\Gamma(3/4)]^2\} = 0.528$  found using quantum Defect Theory (QDT) [31]. The values  $p_{1,0}^{3,2} = 0.54 \pm 0.04$  and  $p_{1,1}^{4,3} = 0.16 \pm 0.02$  for the  $1/R^3$  interaction in the electric field regime have not to our knowledge been determined analytically in a QDT framework.

We also note that these constants barely change between the regime dominated by the van der Waals interaction and the regime dominated by an electric field interaction for the  $|M_L| = 0$  component. The ratio of the  $|M_L| = 1$  to the  $|M_L| = 0$  component in the electric field regime is 0.003. As a consequence, the  $|M_L| = 1$  component is negligible in the electric regime, as seen in Fig. 1 for the LiNa system, and one can provide an estimation of the total  $p$ -wave rate coefficient for the reactive systems by

$$\begin{aligned} \beta_{L=1} &= \beta_{L=1,|M_L|=0} + 2\beta_{L=1,|M_L|=1} \\ &\approx 3\beta_{L=1,|M_L|=0}^{\text{vdW}} + \beta_{L=1,|M_L|=0}^{\text{elec}} \\ &\approx \frac{\pi}{8} \left\{ 0.53 \left( \frac{3^{17} \mu^3 C_6^3}{\hbar^{10}} \right)^{1/4} + 0.54 \left( \frac{2^{9/2} 3^{11/2} \mu^3}{5^3 \hbar^7} \right) \right. \\ &\quad \left. \times \frac{d^6}{(4\pi \epsilon_0)^3} \right\} k_B T \Delta. \end{aligned} \quad (20)$$

## 2. QT model for $s$ -wave collisions

For  $s$ -wave collisions ( $L = 0, M_L = 0$ ), there is no incident barrier because the repulsive centrifugal term vanishes. It is possible, however, to estimate a characteristic length and energy [63] given respectively by

$$a_n = \left( \frac{2\mu C_n}{\hbar^2} \right)^{1/(n-2)}; \quad E_{L=0, M_L=0}^n = \frac{\hbar^2}{2\mu a_n^2}. \quad (21)$$

In the van der Waals regime, the characteristic energy is  $E_{0,0}^6 = \hbar^3 / \sqrt{2^3 \mu^3 C_6}$ . In the electric field regime, the electric dipole-dipole interaction vanishes for  $L = 0$ . But, as there is a coupling between the  $L = 0$  and the  $L = 2$  components in Eq. (8), it is found after diagonalization that the electric dipole interaction behaves as  $-C_4/R^4$  with  $C_4 = 4\mu d^4 / [15\hbar^2 (4\pi \epsilon_0)^2]$  (see Appendix C). In turn, this corresponds to a characteristic energy  $E_{0,0}^4 = 15\hbar^6 (4\pi \epsilon_0)^2 / [16\mu^3 d^4]$ . These results are summarized in Table III.

Substituting these two values of  $E_*$  into Eq. (11) for  $L = 0$ , we arrive at the following expression for the  $L = 0, |M_L| = 0$

TABLE III. Characteristic energies  $E_*$  for  $L = 0, |M_L| = 0$  in the van der Waals (vdW) and electric regimes.

Regime	$ M_L $	$-C_n/R^n$	$E_{L=0,  M_L }^n$
vdW	0	$-\frac{C_6}{R^6}$	$\frac{\hbar^3}{\sqrt{2^3 \mu^3 C_6}}$
Electric	0	$-\frac{4\mu d^4}{15\hbar^2 (4\pi \epsilon_0)^2 R^4}$	$\frac{15\hbar^6}{16\mu^3} \left( \frac{d^2}{4\pi \epsilon_0} \right)^{-2}$

rate as  $d \rightarrow 0$  in the van der Waals regime:

$$\beta_{L=0, |M_L|=0}^{\text{vdW}} = p_{0,0}^6 \pi \left( \frac{2\hbar^2 C_6}{\mu^3} \right)^{1/4} \Delta \quad (22)$$

with

$$p_{0,0}^6 = 1.92 \pm 0.01. \quad (23)$$

The  $L = 0, |M_L| = 0$  rate as  $d \rightarrow d_p$  in the electric field regime is

$$\beta_{L=0, |M_L|=0}^{\text{elec}} = p_{0,0}^4 \pi \frac{\sqrt{16/30}}{\hbar} \frac{d^2}{4\pi \epsilon_0} \Delta \quad (24)$$

with

$$p_{0,0}^4 = 3.74 \pm 0.05. \quad (25)$$

Compared to  $L = 1$ , the rates at ultracold temperature for  $L = 0$  behave now as  $(C_6/\mu^3)^{1/4}$  in the van der Waals regime, making bosonic KRb molecules the least reactive ones and bosonic LiK molecules the most reactive ones, due to the interplay between the  $C_6$  coefficients and the cube of the mass. In the electric field regime, the rates behave as  $d^2$  and are independent of the mass, so that for the same induced dipole all bosonic polar molecules react with the same rate coefficient. The coefficients  $p_{L, |M_L|}^n$  associated with the characteristic energies  $E_{L, |M_L|}^n$  are found by plotting the quantity  $\beta_{L=0, |M_L|=0}^{\text{vdW}}$  obtained from the numerical results of Fig. 2 as a function of the quantity  $(C_6/\mu^3)^{1/4}$  for the van der Waals regime in the top panel of Fig. 4, and the quantity  $\beta_{L=0, |M_L|=0}^{\text{elec}}$  divided by  $d^2$  for the electric regime in the bottom panel of Fig. 4, for the different bosonic reactive systems. As for the fermionic case, the numerical results form a line for the first plot and are constant for the second plot, validating the QT model analysis. Again, we note that the result of  $p_{0,0}^6 = 1.92 \pm 0.01$  in Eq. (23) is in very good agreement with the analytical expression of  $8\pi / [\Gamma(1/4)]^2 = 1.912$  found using quantum defect theory [31] or quantum Langevin theory [37]. The value of  $p_{0,0}^4 = 3.74 \pm 0.05$  agrees within 7% with the analytical expression of 4 from quantum Langevin theory [64] using the  $-C_4/R^4$  interaction in the electric field regime. One can formulate a good approximation for the  $s$ -wave loss rate coefficients by

$$\begin{aligned} \beta_{L=0} &= \beta_{L=0, |M_L|=0}^{\text{vdW}} + \beta_{L=0, |M_L|=0}^{\text{elec}} \\ &\approx \pi \left\{ 1.92 \left( \frac{2\hbar^2 C_6}{\mu^3} \right)^{1/4} + 3.74 \frac{\sqrt{16/30}}{\hbar} \frac{d^2}{4\pi \epsilon_0} \right\} \Delta. \end{aligned} \quad (26)$$

The formulas from Eq. (14) to Eq. (19) and from Eq. (22) to Eq. (25) can be used to determine the inelastic and reactive collisional properties of other atom-atom, atom-molecule, or molecule-molecule collisions, provided that full loss occurs when they encounter one another. This case can occur for molecules of category 2 (NaK, NaRb, NaCs, KCs, RbCs) if the molecules are not in their absolute ground states, for example in higher vibrational states, where inelastic molecule-molecule collision can occur, or when the reactants have higher energy than the products so that an exoergic reaction can take place. Still unknown are the  $C_6$  coefficients (except for RbCs) for each of the initial rovibrational states of these molecules and they have to be calculated individually. For the RbCs and KRb

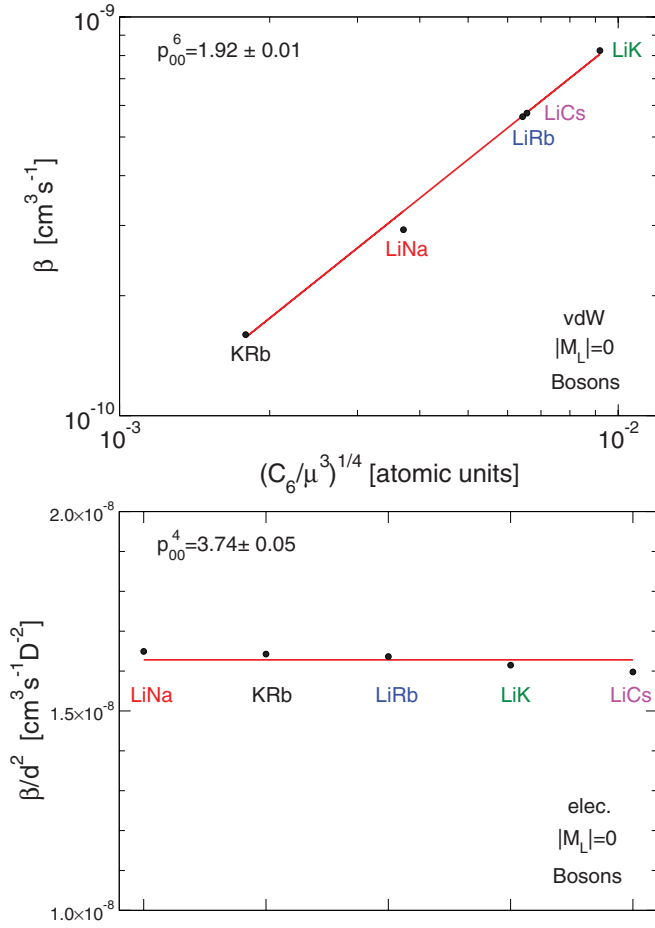


FIG. 4. (Color online) Top panel: van der Waals regime. The quantity  $\beta_{0,0}^6$  is plotted as a function of  $(C_6/\mu^3)^{1/4}$ . Bottom panel: Electric field regime. The quantity  $\beta_{0,0}^4$  divided by  $d^2$  is plotted for the five different colliding species.

molecule the  $C_6$  coefficients have been calculated as functions of the vibrational quantum number in Ref. [33].

We provide in Appendix D the corresponding QT expressions for the imaginary parts of the scattering lengths for  $s$ -wave collisions and scattering volumes for  $p$ -wave collisions.

#### IV. DYNAMICS IN TWO-DIMENSIONAL SPACE

For the confined 2D scattering we use the same formalism developed in Refs. [34,38]. The confinement is given by an optical lattice in the  $\hat{z}$  direction, which we approximate by a harmonic oscillator potential  $V_{\text{ho}} = \mu\omega^2 z^2/2$  of frequency  $\nu$  and angular frequency  $\omega = 2\pi\nu$ . One can also define a harmonic oscillator confinement length  $a_{\text{ho}} = \sqrt{\hbar}/(\mu\omega)$ . We consider the dynamics of two molecules in the ground state of this harmonic oscillator. In confined space,  $M_L$  remains a good quantum number. Additional selection rules apply, and for indistinguishable bosons  $|M_L| = 0$  while for indistinguishable fermions  $|M_L| = 1$  [34,38], for molecules in the ground state of the harmonic confinement. We present in Fig. 5 the loss rate coefficients for a confinement of  $\nu = 20$  kHz as functions of the dipole moment for a given temperature  $T = 500$  nK, for the fermionic species (top panel) and the bosonic species

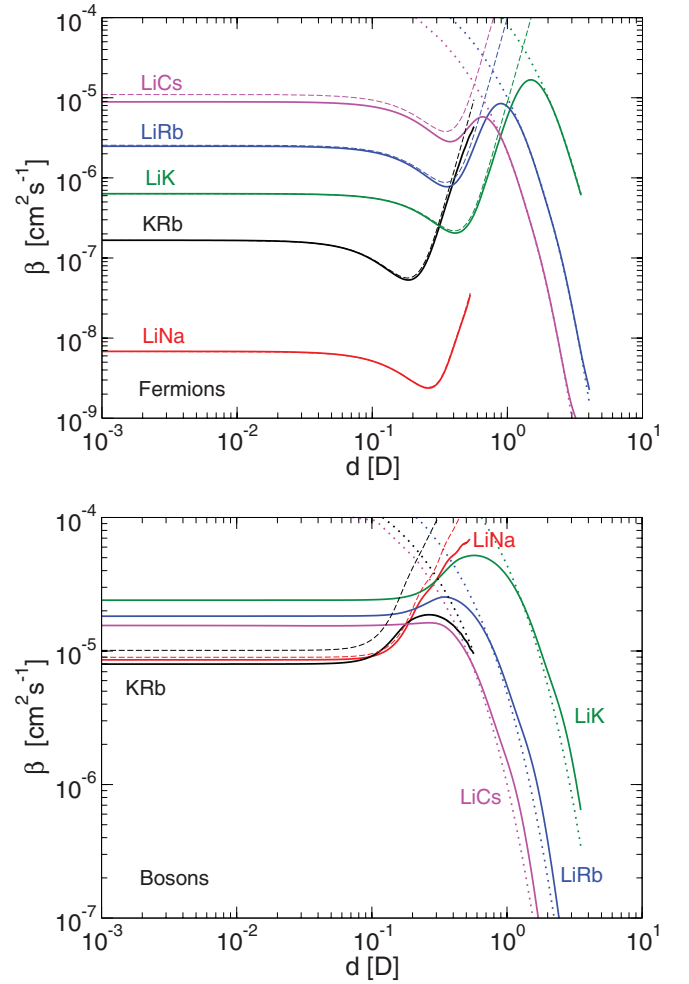


FIG. 5. (Color online) Loss rate coefficients for different reactive polar molecules in confined 2D space, for indistinguishable fermions (top panel) and indistinguishable bosons (bottom panel). The frequency of the 1D trap is  $\nu = 20$  kHz and the temperature is  $T = 500$  nK. The dashed lines represent a model based on the rescaled 3D rate coefficients for  $a_{\text{dd}} \ll a_{\text{ho}}$ , and the dotted lines represent a model based on a functional form (Ref. [40] for example) for  $a_{\text{dd}} \gg a_{\text{ho}}$ .

(bottom panel). We use 40 partial waves,  $L = 1-79$  for the fermions and  $L = 0-78$  for the bosons, to converge the results. At small electric dipoles, when  $a_{\text{dd}} \ll a_{\text{ho}}$ , the collisions are quasi-2D (q2D) and the loss rate coefficients display a similar behavior to that of their 3D counterparts for  $|M_L| = 1$  for the indistinguishable fermions and for  $|M_L| = 0$  for the indistinguishable bosons. At large electric dipoles and for LiK, LiRb, and LiCs, when  $a_{\text{dd}} \gg a_{\text{ho}}$ , the collisions are fully 2D and the loss rate coefficients show a suppression as discussed in Refs. [32,34–36,38–40].

For the quasi-2D regime  $a_{\text{dd}} \ll a_{\text{ho}}$ , we compare using dashed lines in Fig. 5 a two-dimensional loss rate coefficient rescaled from the numerical calculation in three dimensions [35,65,66] from the previous section for  $L = 1$ :

$$\beta^{\text{q2D}} = \frac{3}{2} \frac{\beta^{\text{3D}}}{\sqrt{\pi} a_{\text{ho}}} = \frac{3}{2} \sqrt{\frac{\mu\omega}{\pi\hbar}} \beta^{\text{3D}}, \quad (27)$$

where the factor  $3/2$  accounts for the difference of the mean energies in 3D and 2D for a given temperature  $T$  (in 3D,  $\langle E_c \rangle = 3k_B T/2$  while in 2D,  $\langle E_c \rangle = k_B T$ ). For  $L = 0$ , we get

$$\beta^{q2D} = \frac{\beta^{3D}}{\sqrt{\pi} a_{ho}} = \sqrt{\frac{\mu\omega}{\pi\hbar}} \beta^{3D}. \quad (28)$$

We found for the fermions a good agreement between the numerical 2D rates (shown as solid lines) and the rates rescaled from 3D (dashed lines). For the bosons, a good agreement is found for the LiNa system, but not for the other systems, like KRb for example, even if the order of magnitude is right. For bosons, threshold laws display a logarithmic dependence and are not taken into account in Eq. (28). The QT formulas which describe the numerical 3D rates can also be rescaled in the same manner, so that a good approximation to the loss rate coefficient for fermions in the quasi-2D regime  $a_{dd} \ll a_{ho}$  is given by

$$\begin{aligned} \beta_{L=1}^{q2D} &= 2 \frac{3}{2} \sqrt{\frac{\mu\omega}{\pi\hbar}} \beta_{|M_L|=1}^{3D} \approx 3 \sqrt{\frac{\mu\omega}{\pi\hbar}} \left\{ 0.53 \left( \frac{3^{13} \mu^3 C_6^3}{\hbar^{10}} \right)^{1/4} \right. \\ &\quad \left. + 0.16 \frac{3\pi}{8} \left( \frac{20\,000}{27} \frac{72}{875} \right)^{3/2} \frac{\mu^3}{\hbar^7} \frac{d^6}{(4\pi\epsilon_0)^3} \right\} k_B T \Delta. \end{aligned} \quad (29)$$

For bosons, the rescaled QT formula is

$$\begin{aligned} \beta_{L=0}^{q2D} &= \sqrt{\frac{\mu\omega}{\pi\hbar}} \beta_{|M_L|=0}^{3D} \approx \sqrt{\frac{\pi\mu\omega}{\hbar}} \left\{ 1.92 \left( \frac{2\hbar^2 C_6}{\mu^3} \right)^{1/4} \right. \\ &\quad \left. + 3.74 \frac{\sqrt{16/30}}{\hbar} \frac{d^2}{4\pi\epsilon_0} \right\} \Delta \end{aligned} \quad (30)$$

but is only a good approximation for LiNa.

For the 2D regime  $a_{dd} \gg a_{ho}$ , we compare in Fig. 5 a functional form provided in Refs. [32,35,39,40,67–69]. We found that the forms

$$\beta^{2D} = 2 \times 13 \frac{\hbar}{\mu} \left( \frac{E_c}{\hbar\omega/2} \right)^2 e^{-2(a_{dd}/a_{ho})^{2/5}} \Delta \quad (31)$$

for indistinguishable fermions and

$$\beta^{2D} = 13 \frac{\hbar}{\mu} \left( \frac{E_c}{\hbar\omega/2} \right)^2 e^{-2(a_{dd}/a_{ho})^{2/5}} \Delta \quad (32)$$

for indistinguishable bosons fit well the numerical data. These formulas are reported as dotted lines in Fig. 5. We find the coefficient of 13 in front of the exponential and the coefficient of 2 inside the exponential, by fitting our numerical results. These values are different from the values found in Ref. [40]. This is attributed to the different regimes of collision energies and confinements involved in the fitting. It has been shown in Ref. [40] that the fitting parameters of the functional form may differ for different values of the collision energies.

## V. CONCLUSION

By computing the  $C_6$  coefficients for different pairs of alkali-metal polar molecules of LiNa, LiK, LiRb, and LiCs, and using an available one for KRb, we estimated the quenching rate coefficient assuming full loss when the molecules encounter one another, for the fermionic species

and for the bosonic species, for both the van der Waals and the electric field regimes. We found that, at ultracold temperature, fermionic LiNa is the least reactive system while LiCs is the most in the van der Waals and electric field regimes, due mainly to the increase of the  $C_6$  coefficient for the former regime and the increase of the mass for the latter. Bosonic KRb molecules are found to be the least reactive ones and LiK the most in the van der Waals regime. All the bosonic molecules were found to have the same universal reactive rate in the electric field regime. These behaviors were all explained using a quantum threshold model. From our numerical results, we found analytical expressions for the reactive rate coefficients for fermionic and bosonic molecules, in the van der Waals and electric field regimes. These expressions can be used for other types of system, such as atom-molecule or molecule-molecule collisions assuming full inelastic or reactive loss, if the corresponding  $C_6$  coefficients are known. For example, the analytical expressions can be applied to collision of non-ground-state molecules of NaK, NaRb, NaCs, KCs, and RbCs. The present study provides useful information about collisional properties of heteronuclear alkali-metal polar molecules to which increasing experimental interest is devoted. Future studies will consider the vibrational and rotational dependence of the  $C_6$  coefficient of the heteronuclear alkali-metal molecules, the higher anisotropic terms in the long-range interaction, and the effect of higher collision energy, when more partial waves dominate.

## ACKNOWLEDGMENTS

This material is based upon work supported by the Air Force Office of Scientific Research under the Multidisciplinary University Research Initiative Grant No. FA9550-09-1-0588. A.P. and S.K. also acknowledge funding from NSF Grant No. PHY-1005453.

## APPENDIX A: CHARACTERISTICS OF THE HETERONUCLEAR ALKALI-METAL MOLECULES

We provide in Table IV a summary of the characteristics of the fermionic and bosonic isotopes studied in this work. Conversion factors from atomic units (a.u.) to SI units are as follows: 1 a.u. of mass is equal to 1822.89 amu (atomic mass units), 1 a.u. of electric dipole moment is equal to 2.5417 D, and 1 a.u. of  $C_6$  is equal to  $1 E_H a_0^6$  with  $1 E_H$  (hartree) equal to  $4.359\,743\,94 \times 10^{-18}$  J and  $1 a_0$  (Bohr radius) equal to  $0.529\,177 \times 10^{-10}$  m.

## APPENDIX B: HEIGHT OF THE ADIABATIC BARRIER FOR THE $|M_L| = 1$ COMPONENT IN ELECTRIC FIELD: MIXING $L = 1$ AND $L = 3$

In this case, we have two diabatic effective potential curves,

$$\begin{aligned} V_{L=1}(R) &= \frac{2\hbar^2}{2\mu R^2} - \frac{C_6}{R^6} + \frac{(2/5)d^2}{4\pi\epsilon_0 R^3}, \\ V_{L=3}(R) &= \frac{12\hbar^2}{2\mu R^2} - \frac{C_6}{R^6} - \frac{(2/5)d^2}{4\pi\epsilon_0 R^3} \end{aligned} \quad (B1)$$



TABLE IV. Fermionic (F) or bosonic (B) character, isotope, reduced molecule-molecule mass  $\mu$  (in a.u.),  $C_6$  coefficient (in a.u.), and permanent electric dipole moment  $d_p$  (in D) for the different heteronuclear alkali-metal molecules.

F or B	Isotope	$\mu$ (a.u.)	$C_6$ (a.u.)	$d_p$ (D)
F	$^6\text{Li}^{23}\text{Na}$	26436	3880	0.531
B	$^7\text{Li}^{23}\text{Na}$	27349		
F	$^{40}\text{K}^{87}\text{Rb}$	115638	16133	0.566
B	$^{41}\text{K}^{87}\text{Rb}$	116547		
F	$^7\text{Li}^{40}\text{K}$	42820	524000	3.513
B	$^6\text{Li}^{40}\text{K}$	41907		
F	$^6\text{Li}^{87}\text{Rb}$	84695	1070000	4.046
B	$^7\text{Li}^{87}\text{Rb}$	85608		
F	$^6\text{Li}^{133}\text{Cs}$	126618	3840000	5.355
B	$^7\text{Li}^{133}\text{Cs}$	127531		

and a coupling

$$W(R) = \frac{(2\sqrt{126}/35)d^2}{4\pi\epsilon_0 R^3}. \quad (\text{B2})$$

In the case of  $|W| \ll |V_{L=3} - V_{L=1}|$ , the adiabatic effective potential curves are given after diagonalization by

$$E_{\pm}(R) = V_{L=3/1}(R) \pm \frac{72\mu d^4}{875\hbar^2(4\pi\epsilon_0)^2 R^4}, \quad (\text{B3})$$

and especially the lower one

$$E_{-}(R) = \frac{2\hbar^2}{2\mu R^2} - \frac{C_6}{R^6} + \frac{(2/5)d^2}{4\pi\epsilon_0 R^3} - \frac{C_4}{R^4} \quad (\text{B4})$$

with

$$C_4 = \frac{72\mu d^4}{875\hbar^2(4\pi\epsilon_0)^2}. \quad (\text{B5})$$

At large  $d$ , the most repulsive potential in Eq. (B4) is  $[(2/5)d^2]/[4\pi\epsilon_0 R^3]$  and the most attractive is  $-C_4/R^4$  so that the height of the barrier is

$$E_{L=1, |M_L|=1}^{n=4, m=3} = \frac{(875/24)^3 \hbar^6}{10000\mu^3} \left( \frac{d^2}{4\pi\epsilon_0} \right)^{-2}. \quad (\text{B6})$$

#### APPENDIX C: ADIABATIC POTENTIAL FOR THE $|M_L| = 0$ COMPONENT IN ELECTRIC FIELD: MIXING $L = 0$ AND $L = 2$

Now we have the two diabatic effective potential curves

$$\begin{aligned} V_{L=0}(R) &= -\frac{C_6}{R^6}, \\ V_{L=2}(R) &= \frac{6\hbar^2}{2\mu R^2} - \frac{C_6}{R^6} - \frac{(4/7)d^2}{4\pi\epsilon_0 R^3} \end{aligned} \quad (\text{C1})$$

and the coupling between them

$$W(R) = -\frac{2d^2}{\sqrt{54}\pi\epsilon_0 R^3}. \quad (\text{C2})$$

In the case of  $|W| \ll |V_{L=2} - V_{L=0}|$ , the adiabatic effective

potential curves are given after diagonalization by

$$E_{\pm}(R) = V_{L=2/0}(R) \pm \frac{4\mu d^4}{15\hbar^2(4\pi\epsilon_0)^2 R^4}, \quad (\text{C3})$$

and especially the lower one

$$E_{-}(R) = -\frac{C_6}{R^6} - \frac{C_4}{R^4} \quad (\text{C4})$$

with

$$C_4 = \frac{4\mu d^4}{15\hbar^2(4\pi\epsilon_0)^2}. \quad (\text{C5})$$

#### APPENDIX D: QT EXPRESSION FOR IMAGINARY SCATTERING LENGTHS AND SCATTERING VOLUMES

We provide here the analytical QT expressions for imaginary scattering lengths and imaginary scattering volumes. If we define the scattering length and the scattering volume (see Ref. [70]) by

$$a = a_r - i a_i = -\delta(k)/k, \quad (\text{D1})$$

$$V = V_r - i V_i = -\delta(k)/k^3 \quad (\text{D2})$$

for vanishing wave vectors  $k \rightarrow 0$ , the loss rate can be written as

$$\beta_{L=0} = (4\hbar\pi a_i/\mu)\Delta, \quad (\text{D3})$$

$$\beta_{L=1, M_L} = (4\hbar\pi k^2 V_i/\mu)\Delta$$

for one component  $M_L$ . Similarly, the elastic rate is given by

$$\beta_{L=0}^{\text{el}} = (4\hbar\pi k |a|^2/\mu)\Delta, \quad (\text{D4})$$

$$\beta_{L=1, M_L}^{\text{el}} = (4\hbar\pi k^5 |V|^2/\mu)\Delta.$$

To get the corresponding cross sections, one has to divide the rates by the relative velocity  $v = \hbar k/\mu$ . Identifying the loss rate with the QT model, one gets the imaginary scattering length in the van der Waals regime,

$$a_i = 1.92 \left( \frac{\mu^{1/4} C_6^{1/4}}{2^{7/4} \hbar^{1/2}} \right), \quad (\text{D5})$$

the imaginary scattering length in the electric field regime,

$$a_i = 3.74 \left( \frac{\mu}{\hbar^2 \sqrt{30}} \right) \frac{d^2}{4\pi\epsilon_0}, \quad (\text{D6})$$

the imaginary scattering volume in the van der Waals regime,

$$V_i = 0.53 \left( \frac{3^{9/4} \mu^{3/4} C_6^{3/4}}{32\hbar^{3/2}} \right), \quad (\text{D7})$$

and the imaginary scattering volume in the electric field regime,

$$V_i = 0.54 \left( \frac{3^{9/2} \mu^3}{\hbar^6 2^{1/2} 5^3} \right) \frac{d^6}{(4\pi\epsilon_0)^3}. \quad (\text{D8})$$

In the case of lossy collisions, the imaginary parts  $a_i$  or  $V_i$  contribute to the elastic part of the rates. As a consequence, they provide a minimum value for the elastic rates  $\beta_{L=0}^{\text{el}} = (4\hbar\pi k a_i^2/\mu)\Delta$  for  $s$ -wave collisions and  $\beta_{L=1, M_L}^{\text{el}} = (4\hbar\pi k^5 V_i^2/\mu)\Delta$  for  $p$ -wave collisions. In other words, lossy collisions imply nonzero elastic cross sections or rate coefficients.

- [1] J. M. Sage, S. Sainis, T. Bergeman, and D. DeMille, *Phys. Rev. Lett.* **94**, 203001 (2005).
- [2] E. R. Hudson, N. B. Gilfoy, S. Kotochigova, J. M. Sage, and D. DeMille, *Phys. Rev. Lett.* **100**, 203201 (2008).
- [3] K.-K. Ni, S. Ospelkaus, M. H. G. de Miranda, A. Pe'er, B. Neyenhuis, J. J. Zirbel, S. Kotochigova, P. S. Julienne, D. S. Jin, and J. Ye, *Science* **322**, 231 (2008).
- [4] J. Deiglmayr, A. Grochola, M. Repp, K. Mörtlbauer, C. Glück, J. Lange, O. Dulieu, R. Wester, and M. Weidemüller, *Phys. Rev. Lett.* **101**, 133004 (2008).
- [5] K. Aikawa, D. Akamatsu, M. Hayashi, K. Oasa, J. Kobayashi, P. Naidon, T. Kishimoto, M. Ueda, and S. Inouye, *Phys. Rev. Lett.* **105**, 203001 (2010).
- [6] S. Ospelkaus, K.-K. Ni, G. Quéméner, B. Neyenhuis, D. Wang, M. H. G. de Miranda, J. L. Bohn, J. Ye, and D. S. Jin, *Phys. Rev. Lett.* **104**, 030402 (2010).
- [7] K.-K. Ni, S. Ospelkaus, D. Wang, G. Quéméner, B. Neyenhuis, M. H. G. de Miranda, J. L. Bohn, J. Ye, and D. S. Jin, *Nature (London)* **464**, 1324 (2010).
- [8] M. H. G. de Miranda, A. Chotia, B. Neyenhuis, D. Wang, G. Quéméner, S. Ospelkaus, J. L. Bohn, J. Ye, and D. S. Jin, *Nat. Phys.* **7**, 502 (2011).
- [9] M. Aymar and O. Dulieu, *J. Chem. Phys.* **122**, 204302 (2005).
- [10] J. Deiglmayr, M. Aymar, R. Wester, M. Weidemüller, and Olivier Dulieu, *J. Chem. Phys.* **129**, 064309 (2008).
- [11] B. Deb and L. You, *Phys. Rev. A* **64**, 022717 (2001).
- [12] V. S. Melezhibik and C.-Y. Hu, *Phys. Rev. Lett.* **90**, 083202 (2003).
- [13] P. S. Żuchowski and J. M. Hutson, *Phys. Rev. A* **81**, 060703(R) (2010).
- [14] J. N. Byrd, J. A. Montgomery Jr., and R. Côté, *Phys. Rev. A* **82**, 010502(R) (2010).
- [15] E. R. Meyer and J. L. Bohn, *Phys. Rev. A* **82**, 042707 (2010).
- [16] E. R. Meyer and J. L. Bohn, *Phys. Rev. A* **83**, 032714 (2011).
- [17] S. Ospelkaus, K.-K. Ni, D. Wang, M. H. G. de Miranda, B. Neyenhuis, G. Quéméner, P. S. Julienne, J. L. Bohn, D. S. Jin, and J. Ye, *Science* **327**, 853 (2010).
- [18] G. Quéméner and J. L. Bohn, *Phys. Rev. A* **81**, 022702 (2010).
- [19] C. Ticknor and S. T. Rittenhouse, *Phys. Rev. Lett.* **105**, 013201 (2010).
- [20] Y. Wang, J. P. D’Incao, and C. H. Greene, *Phys. Rev. Lett.* **106**, 233201 (2011).
- [21] Y. Wang, J. P. D’Incao, and C. H. Greene, *Phys. Rev. Lett.* **107**, 233201 (2011).
- [22] L. D. Carr, D. DeMille, R. V. Krems, and J. Ye, *New J. Phys.* **11**, 055049 (2009).
- [23] A. Micheli, G. K. Brennen, and P. Zoller, *Nat. Phys.* **2**, 341 (2006).
- [24] G. Pupillo, A. Micheli, H.-P. Büchler, and P. Zoller, in *Cold Molecules: Theory, Experiment, Applications*, edited by R. V. Krems, W. C. Stwalley, and B. Friedrich (CRC Press, Boca Raton, FL, 2009).
- [25] D. DeMille, *Phys. Rev. Lett.* **88**, 067901 (2002).
- [26] S. F. Yelin, K. Kirby, and R. Côté, *Phys. Rev. A* **74**, 050301(R) (2006).
- [27] A. V. Gorshkov, S. R. Manmana, G. Chen, J. Ye, E. Demler, M. D. Lukin, and A.-M. Rey, *Phys. Rev. Lett.* **107**, 115301 (2011).
- [28] A. V. Gorshkov, S. R. Manmana, G. Chen, E. Demler, M. D. Lukin, and A.-M. Rey, *Phys. Rev. A* **84**, 033619 (2011).
- [29] S. Ospelkaus, A. Pe'er, K.-K. Ni, J. J. Zirbel, B. Neyenhuis, S. Kotochigova, P. S. Julienne, J. Ye, and D. S. Jin, *Nat. Phys.* **4**, 622 (2008).
- [30] S. Kotochigova, E. Tiesinga, and P. S. Julienne, *New J. Phys.* **11**, 055043 (2009).
- [31] Z. Idziaszek and P. S. Julienne, *Phys. Rev. Lett.* **104**, 113202 (2010).
- [32] C. Ticknor, *Phys. Rev. A* **81**, 042708 (2010).
- [33] S. Kotochigova, *New J. Phys.* **12**, 073041 (2010).
- [34] G. Quéméner and J. L. Bohn, *Phys. Rev. A* **81**, 060701(R) (2010).
- [35] A. Micheli, Z. Idziaszek, G. Pupillo, M. A. Baranov, and P. Zoller, and P. S. Julienne, *Phys. Rev. Lett.* **105**, 073202 (2010).
- [36] Z. Idziaszek, G. Quéméner, J. L. Bohn, and P. S. Julienne, *Phys. Rev. A* **82**, 020703(R) (2010).
- [37] B. Gao, *Phys. Rev. Lett.* **105**, 263203 (2010).
- [38] G. Quéméner and J. L. Bohn, *Phys. Rev. A* **83**, 012705 (2011).
- [39] J. P. D’Incao and C. H. Greene, *Phys. Rev. A* **83**, 030702 (2011).
- [40] P. S. Julienne, T. M. Hanna, and Z. Idziaszek, *Phys. Chem. Chem. Phys.* **13**, 19114 (2011).
- [41] C. Haimberger, J. Kleinert, P. Zabawa, A. Wakim, and N. P. Bigelow, *New J. Phys.* **11**, 055042 (2009).
- [42] P. Zabawa, A. Wakim, A. Neukirch, C. Haimberger, N. P. Bigelow, A. V. Stolyarov, E. A. Pazyuk, M. Tamanis, and R. Ferber, *Phys. Rev. A* **82**, 040501(R) (2010).
- [43] A. D. Lercher, T. Takekoshi, M. Debatin, B. Schuster, R. Rameshan, F. Ferlaino, R. Grimm, and H.-C. Nägerl, *Eur. Phys. J D* **65**, 3 (2011).
- [44] M. Debatin, T. Takekoshi, R. Rameshan, L. Reichsöllner, F. Ferlaino, R. Grimm, R. Vexiau, N. Bouloufa, O. Dulieu, and H.-C. Nägerl, *Phys. Chem. Chem. Phys.* **13**, 18926 (2011).
- [45] H. W. Cho, D. J. McCarron, D. L. Jenkin, M. P. Köppinger, and S. L. Cornish, *Eur. Phys. J D* **65**, 125 (2011).
- [46] J. Deiglmayr, M. Repp, A. Grochola, O. Dulieu, R. Wester, and M. Weidemüller, *J. Phys.: Conf. Ser.* **264**, 012214 (2011).
- [47] J. Deiglmayr, M. Repp, O. Dulieu, R. Wester, and M. Weidemüller, *Eur. Phys. J D* **65**, 99 (2011).
- [48] J. Deiglmayr, M. Repp, R. Wester, O. Dulieu, and M. Weidemüller, *Phys. Chem. Chem. Phys.* **13**, 19101 (2011).
- [49] A. Ridinger, S. Chaudhuri, T. Salez, D. R. Fernandes, N. Bouloufa, O. Dulieu, C. Salomon, and F. Chevy, e-print [arXiv:1106.0494](https://arxiv.org/abs/1106.0494).
- [50] A. J. Stone, *The Theory of Intermolecular Forces* (Clarendon Press, London, 1996).
- [51] K. T. Tang, *Phys. Rev.* **177**, 108 (1969).
- [52] R. Barnett, D. Petrov, M. Lukin, and E. Demler, *Phys. Rev. Lett.* **96**, 190401 (2006).
- [53] G. Herzberg, *Spectra of Diatomic Molecules*, 2nd ed. (van Nostrand, Princeton, NJ, 1950).
- [54] J. D. Watts, J. Gauss, and R. J. Bartlett, *J. Chem. Phys.* **98**, 8718 (1993).
- [55] T. H. Dunning Jr., *J. Chem. Phys.* **90**, 1007 (1989).
- [56] B. P. Prascher, D. E. Woon, K. A. Peterson, T. H. Dunning Jr., and A. K. Wilson, *Theor. Chem. Acc.* **128**, 69 (2011).
- [57] Kirk Peterson (private communication).
- [58] I. Lim, P. Schwerdtfeger, B. Metz, and H. Stoll, *J. Chem. Phys.* **122**, 104103 (2005).
- [59] H. A. Bethe, *Phys. Rev.* **47**, 747 (1935).
- [60] E. P. Wigner, *Phys. Rev.* **73**, 1002 (1948).
- [61] R. González-Férez, M. Mayle, P. Sánchez-Moreno, and P. Schmelcher, *Europhys. Lett.* **83**, 43001 (2008).

- [62] J. P. Burke Jr., Ph.D. thesis, University of Colorado, 1999, [<http://jilawww.colorado.edu/pubs/thesis/burke>].
- [63] B. Gao, *Phys. Rev. A* **78**, 012702 (2008).
- [64] B. Gao, *Phys. Rev. A* **83**, 062712 (2011).
- [65] D. S. Petrov and G. V. Shlyapnikov, *Phys. Rev. A* **64**, 012706 (2001).
- [66] Z. Li and R. V. Krems, *Phys. Rev. A* **79**, 050701(R) (2009).
- [67] H. P. Büchler, E. Demler, M. Lukin, A. Micheli, N. Prokofev, G. Pupillo, and P. Zoller, *Phys. Rev. Lett.* **98**, 060404 (2007).
- [68] A. Micheli, G. Pupillo, H. P. Büchler, and P. Zoller, *Phys. Rev. A* **76**, 043604 (2007).
- [69] C. Ticknor, *Phys. Rev. A* **80**, 052702 (2009).
- [70] N. Balakrishnan, V. Kharchenko, R. C. Forrey, and A. Dalgarno, *Chem. Phys. Lett.* **280**, 5 (1997).